

THE LOCAL RATE AND THE PROGENITOR LIFETIMES OF SHORT-HARD GAMMA-RAY BURSTS: SYNTHESIS AND PREDICTIONS FOR THE LASER INTERFEROMETER GRAVITATIONAL-WAVE OBSERVATORY

EHUD NAKAR AND AVISHAY GAL-YAM¹

Division of Physics, Mathematics and Astronomy, California Institute of Technology, 770 South Wilson Avenue,
 MS 103-33, Pasadena, CA 91125; udini@tapir.caltech.edu

AND

DEREK B. FOX

Department of Astronomy and Astrophysics, Pennsylvania State University, 525 Davey Laboratory, University Park, PA 16802

Received 2005 December 5; accepted 2006 April 30

ABSTRACT

The recent discovery of the first four afterglows of short-hard gamma-ray bursts (SHBs) suggests that they typically result from long-lived progenitor systems. The most popular progenitor model invokes the merger of either double neutron star (DNS) binaries or neutron star–black hole (NS-BH) systems. Such events are strong sources of gravitational waves (GWs) and might be detected by ground-based GW observatories. In this work we combine the census of SHB observations with refined theoretical analysis to perform a critical evaluation of the compact binary model. We then explore the implications for GW detection of these events. Beginning from the measured star formation rate through cosmic time, we consider what intrinsic luminosity and lifetime distributions can reproduce the known SHB redshifts and luminosities as well as the peak flux distribution of the large BATSE SHB sample. We find the following: (1) The typical progenitor lifetime is long. Assuming lognormal lifetime distribution, the typical lifetime is >4 (1) Gyr (2σ [3σ] c.l.). If the lifetime distribution is a power law with index η , then $\eta > -0.5$ (-1) (2σ [3σ] c.l.). This result is difficult to reconcile with the properties of the observed Galactic DNS population, suggesting that if SHBs do result from DNS mergers, then the observed Galactic binaries do not represent the cosmic one. (2) We find that the local rate of SHBs is larger than $10 \text{ Gpc}^{-3} \text{ yr}^{-1}$ and may be higher by several orders of magnitude, significantly above previous estimates. (3) Assuming that SHBs do result from compact binaries, our predictions for the LIGO and VIRGO event rates are encouraging: the chance for detection by current facilities is not negligible, while a coincident detection of GW and electromagnetic radiation from an SHB is guaranteed for next-generation observatories.

Subject headings: gamma rays: bursts — gravitational waves

Online material: color figures

1. INTRODUCTION

More than a decade ago it was realized that gamma-ray bursts (GRBs) can be divided into two well-defined subpopulations: the majority of the observed bursts (about $\frac{3}{4}$) had durations longer than ~ 2 s and relatively softer observed spectra, and the minority ($\sim \frac{1}{4}$) had short durations and harder observed spectra (Kouveliotou et al. 1993). Accordingly, the two components of this bimodal population are often referred to as long-soft GRBs and short-hard GRBs (SHBs hereafter).

Observational evidence accumulated in the last few years has conclusively shown that long-soft GRBs are associated with supernovae (SNe) and result from the death of short-lived massive stars (Galama et al. 1998; Kulkarni et al. 1998; Bloom et al. 1999b, 2002; Stanek et al. 2003; Hjorth et al. 2003; Matheson et al. 2003; Lipkin et al. 2004; Gal-Yam et al. 2004; Malesani et al. 2004; Cobb et al. 2004; Thomsen et al. 2004; Soderberg et al. 2005). Comparable studies of SHBs were not conducted due to observational difficulties in obtaining accurate localizations for these events.

A breakthrough in the study of SHBs occurred earlier this year when the *Swift*² and *HETE-2*³ satellites provided the first timely and accurate localizations of SHBs 050509b, 050709, and 050724,

leading to the detection of afterglow emission in X-ray, optical, IR, and radio wavelengths, as well as to the identification and study of the host galaxies of these events (Bloom et al. 2006; D. B. Fox et al. 2006, in preparation; Gehrels et al. 2005; Castro-Tirado et al. 2005b; Prochaska et al. 2005; Fox et al. 2005; Hjorth et al. 2005a, 2005b; Covino et al. 2006; Berger et al. 2005). These studies provide three strong indications that SHBs result from a different type of physical progenitor system. First, in all three events there are no indications of an associated SN, to within strict limits. SNe similar to those associated with long-soft GRBs would have been easily detected. Second, two of these events occurred within early-type galaxies, with little or no recent star formation. None of the many tens of long-soft GRBs with comparable data are detected in such galaxies. Finally, all of these bursts occurred relatively nearby, at redshifts $z < 0.3$, in contrast with long GRBs that are typically at $z > 1$. Taken together these observational facts strongly indicate that SHBs have a different type of progenitor system and that some of these progenitors are long lived ($\gtrsim 1$ Gyr).

The most popular model (e.g., Eichler et al. 1989; Narayan et al. 1992) for SHBs invokes the merger of two compact objects, such as double neutron stars (DNSs) or a neutron star and a black hole (NS-BH). Such models are appealing because they predict events with comparable timescale and energy release to those observed in short bursts. Such considerations, combined with the recent results showing that SHBs require a long-lived progenitor system,

¹ Hubble Fellow.

² See <http://swift.gsfc.nasa.gov/docs/swift/swiftsc.html>.

³ See <http://space.mit.edu/HETE/Welcome.html>.

led several groups to suggest that SHBs result from compact binary mergers (e.g., Bloom et al. 2006; Fox et al. 2005; Berger et al. 2005). More detailed comparisons with model predictions were limited by the small numbers of SHBs with known host galaxies and redshifts.

Gal-Yam et al. (2005) have expanded the sample of SHBs available for study using new and archival observations of “historical” SHBs, allowing them to establish a statistically significant association between two additional SHBs (790613 and 000607) and their probable host galaxies or clusters. Combining these data with observations of the recent *Swift* and *HETE-2* SHBs discussed above, as well as an additional *Swift* burst (SHB 050813) possibly located in a $z = 0.72$ galaxy cluster (Gladders et al. 2005; Berger 2005; Prochaska et al. 2005), Gal-Yam et al. (2005) confronted predictions from binary NS merger models (Ando 2004; Guetta & Piran 2005) with the properties of the observed SHB sample. They found that the model predictions are difficult to reconcile with the properties of the observed SHB sample, since the range of models considered in the literature inevitably predicts a large fraction of short-lived merging systems, which will preferably reside in late-type hosts and occur at higher redshifts, in contrast with the observed SHB sample, which is dominated by events located in early-type hosts and at lower redshifts.

In this work we apply a refined theoretical analysis to the Gal-Yam et al. (2005) sample in order to constrain the local rate and the lifetime of SHB progenitors. Our goal is to confront our findings with compact binary models for SHBs and discuss the implication for gravitational wave (GW) detection from SHBs by the LIGO and VIRGO observatories.

The structure of the paper is as follows: We develop the theory that we need for the analysis of the data in § 2. The observed sample, its analysis, and the derived constraints are presented in § 3. We compare our results to the predictions of compact binary mergers in § 4 and discuss the prospects for detecting GWs from SHBs under the assumption that they originate from a DNS or BH-NS mergers in § 5. We summarize our conclusions in § 6.

2. THEORY

We use the combination of the two-dimensional *observed* redshift and luminosity distribution together with the observed SHB flux distribution ($\log N - \log S$), to constrain the *intrinsic* SHB rate at redshift z , $R_{\text{SHB}}(z)$, and the intrinsic luminosity function $\phi(L)$. This method is an extension of previous works (Piran 1992; Ando 2004; Guetta & Piran 2005) that used only the one-dimensional observed redshift distribution and the peak flux distribution. Although we focus here on SHBs, the method is applicable to long-soft GRBs as well.

The two-dimensional observed redshift and luminosity distribution is derived from the intrinsic distributions via

$$\frac{d\dot{N}_{\text{obs}}}{dL dz} = \phi(L) \frac{R_{\text{SHB}}}{1+z} \frac{dV}{dz} S(P), \quad (1)$$

where \dot{N}_{obs} is the *observed* SHB rate and $\phi(L)$ is the *intrinsic* peak luminosity function (which we assume to be independent of z). Here $0 < S(P) < 1$ is the probability for detection (including redshift determination) of a burst with a peak photon flux P , which in turn depends on L and z , as well as on the spectrum of the bursts. $R_{\text{SHB}}(z)$ is the intrinsic SHB rate per unit comoving volume and comoving time. Since SHB progenitors are most likely of a stellar origin, we expect

$$R_{\text{SHB}}(z) \propto \int_z^\infty \text{SFR}(z') f(t(z) - t(z')) \frac{dt}{dz'} dz', \quad (2)$$

where $\text{SFR}(z)$ is the star formation rate at redshift z (per unit comoving volume and comoving time), $t(z)$ is the age of the universe at redshift z , and $f(\tau)$ is the fraction of SHB progenitors that are born with a lifetime τ .

$S(P)$ can describe a single detector or a combination of several detectors, each weighted by its field of view and operational time. In principle, if $S(P)$ is well known and if the observed sample is large enough, then the intrinsic distributions can be extracted from equation (1). In reality we have to work with a limited sample, as well as poorly understood $S(P)$. In the case of GRBs (long and short) there is a large sample of bursts, observed by BATSE,⁴ for which only the peak flux distribution is available while the redshift (and thus luminosity) is unknown. The BATSE sample can constrain the intrinsic distributions by considering the observed flux distribution, which is an integration of equation (1):

$$\frac{d\dot{N}_{\text{obs}}}{dP} = \frac{d}{dP} \int_0^\infty dz \int_{L_{\min}(z, P)}^\infty dL \frac{d\dot{N}}{dL dz}, \quad (3)$$

where

$$L_{\min}(z, P) = 4\pi d_L^2 k(z) P, \quad (4)$$

$d_L(z)$ is the luminosity distance, and $k(z)$ depends on the spectrum of the bursts and includes the k -correction and the conversion from energy flux to photon flux. Parameter $k(z)$ is assumed to be a function of the redshift only. Note that the $\log N - \log S$ distribution is $\dot{N}(>P)$ in our notation.

If $\phi(L)$ is a single power law, $\phi(L) = \phi_0 L^{-\beta}$, with no upper or lower cutoff (within a luminosity range that we discuss below), then the integral over z in equation (3) does not depend on P and thus the observed peak flux distribution does not depend on R_{SHB} and simply satisfies

$$\frac{d\dot{N}_{\text{obs}}(P)}{dP} \propto P^{-\beta} S(P). \quad (5)$$

Similarly, the integral over L in equation (1) results in

$$\frac{d\dot{N}_{\text{obs}}}{dz} = [4\pi d_L^2 k(z)]^{1-\beta} \phi_0 \frac{R_{\text{SHB}}}{1+z} \frac{dV}{dz} \int P^{-\beta} S(P) dP, \quad (6)$$

thereby eliminating the dependence on the detector thresholds. Naturally for $\beta < 2$ an upper cutoff must exist while for $\beta > 1$ a lower limit is necessary. However, if the lower cutoff is low enough so that it affects only a negligible volume, and if the upper cutoff is high enough so that it affects only the detection at high redshift, then equations (5) and (6) are applicable (these cutoffs also prevent the integral over P in eq. [6] from diverging). Therefore, if the observed peak flux distribution can be fitted by equation (5), then the luminosity function can be a single power law. In this case we can readily use data sets for which $S(P)$ is not well known. In such cases equation (6) enables a comparison of the one-dimensional observed redshift distribution with model predictions. Unfortunately the *observed* luminosity distribution depends on $S(P)$ even when the luminosity function is a single power law. If $S(P)$ is well known, a better constraint on the intrinsic distributions can be obtained by a comparison with the two-dimensional luminosity-redshift distribution (eq. [1]).

The above formalism is applicable to any astrophysical transient as long as its detectability depends only on its peak flux. Equations (1) and (3) are the most general, assuming only that the luminosity function does not evolve with the redshift. Equations (5)

⁴ See <http://www.batse.msfc.nasa.gov/batse/>.

TABLE 1
HOST GALAXIES AND REDSHIFTS OF SHBs

SHB	Redshift z	Host Galaxy Type	Association Significance	References
790613.....	0.09	E/S0	$\sim 3 \sigma$	1
000607.....	0.14	Sb	$\sim 2 \sigma$	1
050509b.....	0.22	E/S0	$3-4 \sigma$	2
050709.....	0.16	Sb/c	Secure	3
050724.....	0.26	E/S0	Secure	4
050813.....	0.72 ^a	E/S0	...	5
001204.....	>0.25 (0.06)	...	1σ (2σ)	1
000607.....	>0.25 (0.06)	...	1σ (2σ)	1

^a While the paper was in the referring process, Berger (2006) suggested that this burst might be actually associated with a cluster at a redshift ≈ 1.8 .

REFERENCES.—(1) Gal-Yam et al. 2005; (2) Bloom et al. 2006; D. B. Fox et al. 2006, in preparation; Castro-Tirado et al. 2005a; Gehrels et al. 2005; (3) Fox et al. 2005; (4) Berger et al. 2005; Prochaska et al. 2005; (5) Gladders et al. 2005; Berger 2005; Prochaska et al. 2005.

and (6) are applicable only when the luminosity function is a single power law and $k(z)$ depends only on the redshift.

3. CONSTRAINTS ON PROGENITOR LIFETIME AND THE RATE OF SHBs

In this section we use the methods presented in § 2 to analyze the observed sample of SHBs. We base our study on the SHB sample compiled by Gal-Yam et al. (2005). This sample includes four relatively recent SHBs localized by *Swift* and *HETE-2* and four “historical” bursts localized by the Interplanetary Network (IPN) over the years and studied in retrospect by these authors. We summarize the known redshift and host galaxy properties of each burst, as compiled by Gal-Yam et al. (2005), in Table 1.

When using this sample for statistical studies of the observed redshifts, as we do here, one has to account for selection biases. Specifically, a selection bias that disfavors the identification of the host galaxy of an SHB at high redshift may skew our results. Fortunately, the sample we use is almost complete, making correction for selection biases simple. At the time that the analysis was first made *Swift* had detected and made prompt follow-up observations of only four SHBs. Three are included in our sample while the last (SHB 050906) might be associated with a galaxy at a distance of 140 Mpc (Levan & Tanvir 2005). If correct, this low redshift strengthens our results, as seen below; however, we do not include this burst due to the association being unconfirmed at this time.⁵

The four IPN SHBs studied by Gal-Yam et al. (2005) comprise a complete subsample of IPN SHBs localized to within 10 arcmin², defined by these authors based on a priori technical issues (e.g., Galactic latitude), which should not bias the physical properties of these bursts. Of these four bursts, Gal-Yam et al. (2005) determine probable redshifts and host galaxy types for two events. For the other two events they set a lower redshift limit. This limit is based on a null detection of luminosity overdensities in the fields of these SHBs, and thus no host galaxy information is available. Since Gal-Yam et al. (2005) used a luminosity-based test for associating hosts with SHBs, their search may be biased against bursts in low-luminosity galaxies and against bursts at high red-

shift. To avoid the bias mentioned above, our statistical analysis is based on the density distributions derived from the lower limits on the redshift of these two bursts (see § 3.1).

We use the observed peak flux sample in the current BATSE catalog.⁶ Therefore, it is convenient to define the flux and intrinsic luminosity quantities discussed in § 2 in an energy range that corresponds to the BASTE window for detection, 50–300 keV. In this window the spectrum can be well approximated as a single power law $F_\nu \propto \nu^{-\alpha}$ where values range between $-1 < \alpha < 0.5$ (Ghirlanda et al. 2004) with a typical value $\alpha \approx -0.5$. Using this spectrum, we obtain $k(z) \approx 2 \times 10^{-7} (1+z)^{-(1-\alpha)}$ ergs.

3.1. The Progenitor Lifetime of SHBs

3.1.1. Single Power-Law Luminosity Functions

Following the discussion in § 2, we first try to fit the observed peak flux distribution $dN(P)/dP$ using a single power law with an index β . From the current BATSE catalog we extract all of the short ($T_{90} < 2$ s) bursts with peak flux in the 64 ms timing window of $P_{64} > 1.5$ photons cm⁻² s⁻¹ [at this range $S(P) \approx 1$ for BATSE], resulting in a list of 340 bursts. We calculate the maximum likelihood and find that $\beta = 2 \pm 0.1$ provides the best fit. The χ^2/dof of this model is 1.17, confirming that it is indeed a good fit. Using equation (5), we therefore initially consider a single power-law luminosity function $\phi(L) \propto L^{-2}$.

The eight SHBs with known (or constrained) redshifts included in our sample were detected by several different instruments (see Table 1). The detection threshold for each experiment is not well known and construction of $S(P)$ for this sample is therefore currently impossible. Hence, the full sample can be used only for comparison with models of the redshift distribution based on a single power-law luminosity function. Should a larger sample of bursts for which the detector sensitivity is well understood become available in the future, the more constraining comparison with model predictions using the two-dimensional L - z distribution (eq. [1]) could be carried out.

Following Schmidt (2001) and Guetta & Piran (2005), we base our redshift distribution model calculations on the star formation history (SFH) parameterization SF2 of Porciani & Madau (2001),

$$\text{SFR}_2(z) \propto \frac{\exp(3.4z)}{\exp(3.4z) + 22} \frac{[\Omega_m(1+z)^3 + \Omega_\Lambda]^{1/2}}{(1+z)^{3/2}}, \quad (7)$$

and we adopt the standard cosmology ($\Omega_m = 0.3$, $\Omega_\Lambda = 0.7$, and $H_0 = 70$ km s⁻¹ Mpc⁻¹). The probability distributions we consider for the lifetime are lognormal, $f(\tau) d\tau = [\tau\sigma(2\pi)^{1/2}]^{-1} \exp\{-[\ln(\tau) - \ln(\tau_*)]^2/2\sigma^2\} d\tau$ with various values of τ_* and narrow ($\sigma = 0.3$) or wide ($\sigma = 1$) dispersions, as well as power-law distributions $f(\tau) \propto \tau^{-\eta}$ with a lower cutoff at 20 Myr and an upper cutoff that is larger than the Hubble time (our results do not depend on the exact values of the cutoffs). For each of these models we carry out a maximum likelihood analysis (Press et al. 1992) in order to constrain the typical delay (τ_*) or power-law index (η). We do so by calculating the likelihood of the observations (Table 1) for every set of model predictions (calculated using eqs. [6] and [7]). The two bursts with redshift lower limits are accounted for in the following way. For each burst we calculate the functional form of the lower limit, $l(z)$, which is defined as 1 minus the significance level in which the hypothesis that the burst is at redshift z is rejected. So, $l(z)$ goes to 1 for high redshifts (the possibility that these bursts are at high z is not constrained), and $l(z)$ decreases with z , for example,

⁵ During the refereeing process *Swift* localized an additional handful of SHBs. For most of these bursts there is currently no redshift or host information. For SHB 051221 the redshift and host are known (Soderberg et al. 2006). We stress that this burst, or future bursts, cannot be added to a sample that is used in a statistical comparison to the observations without proper consideration of the selection effects that prevented the redshift determination of the rest of the localized SHBs.

⁶ See <http://www.batse.msfc.nasa.gov/batse/grb/catalog/current/>.

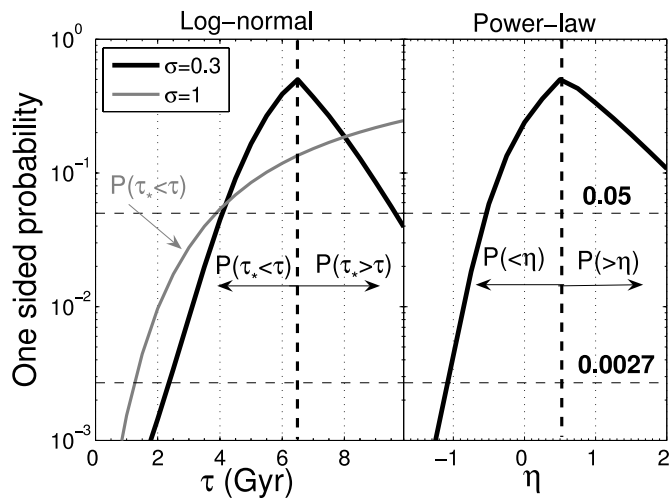


FIG. 1.—*Left*: One-sided probability curves, which result from the maximum likelihood analysis, for narrow (thick line) and wide (thin line) lognormal lifetime distributions. For lifetime values, τ , that are smaller (larger) than the most probable value, the one-sided probability is the probability that $\tau_* < \tau$ ($\tau_* > \tau$). For the most probable value this probability is 0.5. Considering a narrow lognormal distribution, the most likely delay is $\tau_* = 6.5$ Gyr and its 5%–95% confidence interval is 4 Gyr $< \tau_* < 9.5$ Gyr, while the probability that $\tau_* > 1$ Gyr is 99.98%. Assuming a wide lognormal distribution, the most likely delay is $\tau_* = 20$ Gyr while $\tau_* > 4$ (1) Gyr at 95% (99.9%). *Right*: One-sided probability curves of a single power-law lifetime distribution. The most probable power-law index is $\eta = 0.6$, the 5%–95% confidence interval is $-0.5 < \eta < 2.6$, and the probability that $\eta > -1$ is 99.5%. See § 3.1.1 for details. [See the electronic edition of the Journal for a color version of this figure.]

assuming the value 0.05 at $z = 0.06$ (Table 1). The method used to calculate $l(z)$ is described in detail in Nakar et al. (2006) and is applied to these bursts in Gal-Yam et al. (2005). The likelihood of a burst with a lower limit is the probability that an observed burst will be consistent with the observed lower limit for a given model of redshift distribution: $\int (dN_{\text{obs}}/dz)l(z) dz$.

The results of the likelihood analysis that we carry out for the different lifetime distributions are presented as one-sided probability curves in Figure 1. For a model likelihood \mathcal{L} the one-sided probability is defined as $\{1 - P_{\chi^2,1}[2 \ln(\mathcal{L}_{\text{max}}/\mathcal{L})]\}/2$, where \mathcal{L}_{max} is the maximal likelihood and $P_{\chi^2,1}$ is the cumulative χ^2 distribution with 1 degree of freedom (e.g., Press et al. 1992). Figure 1 shows clearly that long lifetimes are favored. For the narrow lognormal distribution we find that the most likely delay is $\tau_* = 6.5$ Gyr and its 5%–95% confidence interval is 4 Gyr $< \tau_* < 9.5$ Gyr, while the probability that $\tau_* > 1$ Gyr is 99.98%. Assuming a wide lognormal distribution, we find that the most likely delay is larger than the Hubble time ($\tau_* = 20$ Gyr), that $\tau > 4$ Gyr at 95% confidence, and that the probability that $\tau_* > 1$ Gyr is 99.9%. Considering a power-law lifetime distribution, we find that the most probable power-law index is $\eta = 0.6$, the 5%–95% confidence interval is $-0.5 < \eta < 2.6$, and the probability that $\eta > -1$ is 99.5%.⁷

The normalized (*intrinsic*) redshift distributions, $R_{\text{SHB}}(z)$, resulting from various lifetime distributions are presented in Figure 2. Comparison between the predicted and observed cumulative redshift distributions for several representative models is depicted in

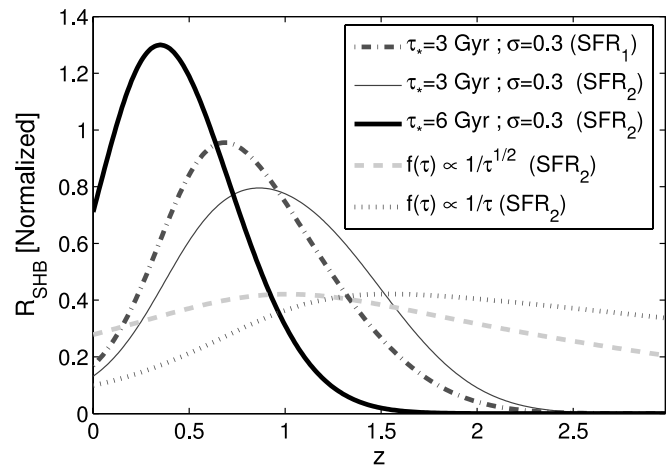


FIG. 2.—Normalized intrinsic SHB rate (R_{SHB}) as a function of the redshift for several lifetime distributions and SFH parameterizations (see inset). [See the electronic edition of the Journal for a color version of this figure.]

Figure 3. This figure vividly illustrates the results from our maximum likelihood analysis, namely, that models consistent with the data must have a long typical delay (≥ 4 Gyr). Models with no typical lifetime (power-law distributions) must have a birthrate of progenitors per unit logarithmic lifetime that increases significantly as a function of lifetime (i.e., $\eta > -0.5$). This figure also shows that indeed all of the models we considered provide a good fit to the data when $\tau_*(\eta)$ takes its most likely value. It also demonstrates that the reason that models dominated by short-lived systems are rejected is that they underpredict the fraction of bursts at low redshift ($z \lesssim 0.3$).

Given that the sample that we use is small, and to test for biases in our maximum likelihood analysis, we have carried out a jack-knife analysis (Efron 1982). Namely, we repeat the analysis eight times, in each occasion removing a different burst from the sample (i.e., using a different sample of seven bursts). We find a negligible

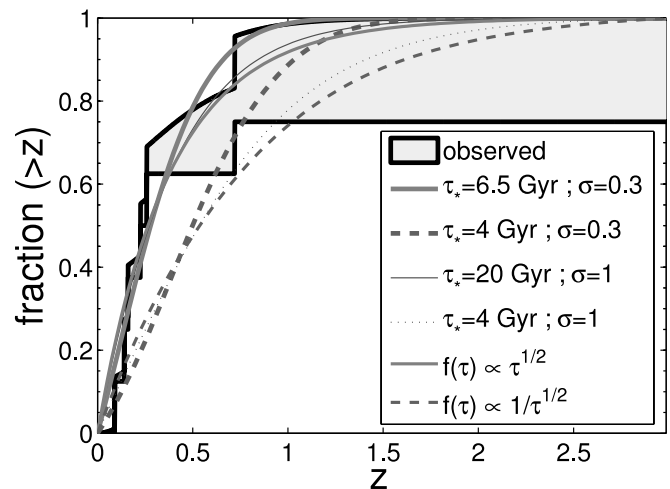


FIG. 3.—Cumulative observed redshift distribution as predicted by various lifetime distributions when the luminosity function is $\phi(L) \propto L^{-2}$ and the SFH is given by eq. (7). For each functional form of the lifetime distribution we present the most likely distribution and the distribution that is rejected at 95% confidence level. The cumulative redshift distribution of the observed data (shaded region) is bracketed between the lower solid line, which is the cumulative redshift distribution of the six bursts with known redshifts, and the upper solid line, which includes also the contribution of the two bursts with upper limits, as given by $l(z)$ (see text). The figure demonstrates that the most likely models provide a good fit to the data while the models that are rejected underpredict the fraction of bursts at low redshift $z \lesssim 0.3$. [See the electronic edition of the Journal for a color version of this figure.]

⁷ In these calculations we took the redshift of SHB 050813 as 0.72 (Gladders et al. 2005; Berger 2005; Prochaska et al. 2005). While the paper was in the refereeing process, Berger (2006) suggested that this burst might actually be associated with a cluster at a redshift higher than 0.72. Repeating the analysis while taking a lower limit of $z > 0.72$ for SHB 050813 does not change the results significantly. For example, for narrow lognormal distribution, the most likely delay is $\tau_* = 5.8$ Gyr, the 5%–95% confidence interval is 3.5 Gyr $< \tau_* < 9$ Gyr, while the probability that $\tau_* > 1$ Gyr is 99.8%.

bias, for example, the bias of the most likely τ_* (η) for a narrow lognormal (power-law) distribution is -0.05 Gyr (0.15), implying that the most likely values that are obtained by the maximum likelihood analysis are not biased because of the small sample size. We also find that our results are not driven by any single burst. For example, for a narrow lognormal lifetime distribution the most likely value of τ_* in the different samples varies between 5.8 and 8 Gyr (in the full sample it is 6.5 Gyr), and in all of the samples $\tau_* > 3.4$ Gyr at more than 95% c.l. while the probability that $\tau_* > 1$ Gyr is, in all samples, higher than >99.8%.

Given the observational uncertainty in the SFH at high redshift, we repeat our analysis using the SFH formula SF1 from Porciani & Madau (2001):

$$\text{SFR}_1(z) \propto \frac{\exp(3.4z)}{\exp(3.8z) + 45} \frac{[\Omega_m(1+z)^3 + \Omega_\Lambda]^{1/2}}{(1+z)^{3/2}}. \quad (8)$$

In this model the star formation rate falls exponentially at redshifts larger than 1.5. The results we obtain using this SFH model are similar to those obtained using equation (7). For example, considering a narrow lognormal distribution with SFR_1 , we find that the most likely delay is $\tau_* = 6$ Gyr and its 5%–95% confidence interval is $3.5 \text{ Gyr} < \tau_* < 9 \text{ Gyr}$ while the probability that $\tau_* > 1$ Gyr is 99.95%. The reason is that the models differ only at high redshift, with little impact on the distribution at low redshifts. Of the three models presented in Porciani & Madau (2001) this model places the most conservative constraints on $f(\tau)$ as it predicts the largest fraction of SHBs at low redshift (for a given lifetime distribution). Therefore, lifetime distributions that are ruled out when applied to this model will be ruled out with greater significance when the other Porciani & Madau (2001) SFH models are used.

We return now to the upper and lower cutoffs of the luminosity function. As described above, for a given selection of R_{SHB} and $S(P)$ there are critical values of the lower (upper) luminosity function cutoffs, below (above) which the observations are insensitive to the value of the cutoff. Among all of the models of R_{SHB} that we have examined, and for threshold values that vary between⁸ 1 and 50 photons $\text{cm}^{-2} \text{ s}^{-1}$, the fit to the $\log N - \log S$ distribution, as well as the fit to the observed redshift distribution, is insensitive to a lower cutoff $L_{\min} < 10^{49} \text{ ergs s}^{-1}$ and to an upper cutoff $L_{\max} > 10^{52} - 10^{53} \text{ ergs s}^{-1}$. Namely, a luminosity function with $\phi(L) \propto L^{-2}$ for $10^{49} \text{ ergs s}^{-1} < L < 10^{53} \text{ ergs s}^{-1}$ and $\phi(L) = 0$ otherwise is consistent with all available data. The luminosity of every SHB in our sample falls within this range as well. Although the sample that we consider is consistent with $L_{\min} = 10^{49} \text{ ergs s}^{-1}$, recent results suggest a lower L_{\min} . First, if SHB 050906 is associated with the nearby galaxy IC 328 at 140 Mpc, as suggested by Levan & Tanvir (2005), then its luminosity is about $10^{48} \text{ ergs s}^{-1}$. Second, Tanvir et al. (2005) found evidence that at least 5% of the SHBs detected by BATSE are at $z < 0.025$ (≈ 100 Mpc). Interestingly, a comparable fraction ($\approx 5\%$) is predicted by our best-fit model [$\phi(L) \propto L^{-2}$ and a typical lifetime of 6 Gyr] if the lower cutoff is as low as $L_{\min} < 10^{46} \text{ ergs s}^{-1}$. A slightly smaller, but consistent, fraction ($\approx 3\%$) is predicted if $L_{\min} = 10^{47} \text{ ergs s}^{-1}$, while the fraction drops to less than 0.5% for $L_{\min} = 10^{48} \text{ ergs s}^{-1}$.

If $L_{\min} \lesssim 10^{47} \text{ ergs s}^{-1}$, then the SHB luminosity function overlaps with the energies observed in giant flares from soft gamma-ray repeaters (SGRs; Hurley et al. 2005; Palmer et al. 2005). This overlap in luminosities raises (again) the question of whether SGRs

can produce flares with isotropic equivalent observed luminosities much greater than $\sim 10^{47} \text{ ergs s}^{-1}$, as we previously suggested in Nakar et al. (2006). In this case giant flares from SGRs can be the source of all observed SHBs (Dar 2005a). The fact that SHBs are observed in elliptical galaxies cannot a priori rule out this possibility since it might be that neutron stars (and thus SGRs) can still be produced long after star formation ended in such galaxies (Dar 2005b). For example, it has been proposed that neutron stars can be the end product of white dwarf binary mergers (Saio & Nomoto 1985) or of an accretion-induced collapse of a white dwarf (Nomoto & Kondo 1991). However, observations indicate that SGRs and anomalous X-ray pulsars (AXPs), two known populations of magnetar candidates in our Galaxy, are associated with star-forming regions (Gaensler et al. 2001). Thus, our result that SHBs are dominated by progenitors with a lifetime of several billion years disfavors this possibility.

3.1.2. Broken Power-Law Luminosity Functions

Although a broken power-law luminosity function is not necessary in order to explain the data, this, or even more complicated functional forms, cannot be excluded. Given the prominence of broken power-law luminosity functions in previous studies, we also consider a luminosity function of the form

$$\phi(L) \propto \begin{cases} L^{-\alpha_1}, & L < L_*, \\ L^{-\alpha_2}, & L > L_*, \end{cases} \quad (9)$$

where $\alpha_1 < 1.5$ and $\alpha_2 > 2.5$. We choose this range of indices so the luminosity function will significantly deviate from the single power law for which we already obtained a constraint on the lifetime. Another reason for exploring a broken power-law distribution is that it demonstrates the analysis that should be done once the sample of *Swift* short bursts with known redshift is significantly larger and the *Swift* threshold is better understood. Such luminosity functions couple the intrinsic functions to the detector response when equation (1) is integrated over L or z . Therefore, in this case, $S(P)$ needs to be understood in order to compare the observations with the model. Since we cannot construct $S(P)$ for the whole sample, we use in this section only the three bursts detected by *Swift*. However, as we now account for $S(P)$ (and its uncertainties), we can use the two-dimensional distribution (eq. [1]). Based on the peak flux of the three *Swift* SHBs with known redshifts, we estimate the *Swift* BAT threshold for localizations to be comparable to that of BATSE. We therefore approximate *Swift*'s threshold as a step function at 1 photon $\text{cm}^{-2} \text{ s}^{-1}$ with a large uncertainty due to the small number of *Swift* SHBs. We use equation (7) for the SFH.

In order to test the effect of broken power-law luminosity functions on the derived limits on the lifetime, we carry out a maximal likelihood analysis for the narrow lognormal and the single power-law lifetime distributions. For each model we first fix $\alpha_1 = 1.5$ and $\alpha_2 = 2.5$ and fit L_* to the BATSE $\log N - \log S$ distribution. A narrow lognormal lifetime distribution results with a most likely delay of $\tau_* = 6.5$ Gyr and $\tau_* > 4$ (1) Gyr at 95% (99.98%). A power-law lifetime distribution results with a most likely power-law index of $\eta = 1$ and with $\eta > 0$ (-1) at 95% (99.9%). Repeating the analysis with other values of α_1 and α_2 (fitting L_* to the BATSE $\log N - \log S$ distribution), we obtain similar results. Given the uncertainty in the *Swift* threshold, we have also varied the assumed threshold value by a factor of 5 below our best estimate (retaining its step function form), again finding similar results. Note that although here we can use a significantly smaller sample (three bursts) than the one we used in § 3.1.1 (eight bursts), we obtain similar significance. The reason is, at least partially, the usage

⁸ This range includes the estimated thresholds of all of the instruments that contributed to the detection of our SHB sample.

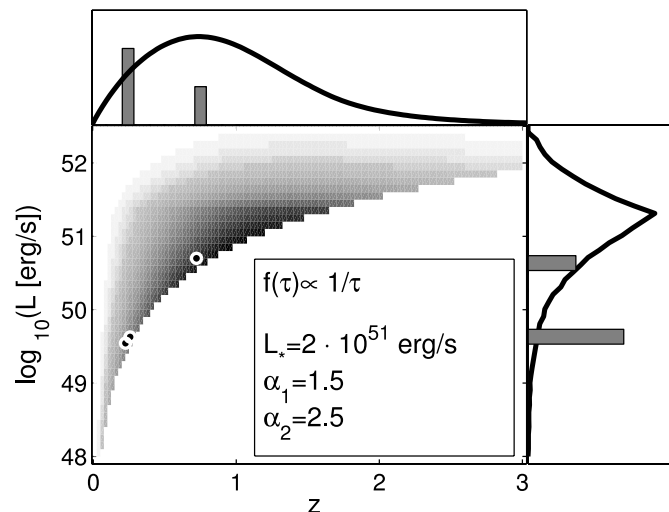


FIG. 4.—Plot of the two-dimensional distribution $d\dot{N}_{\text{obs}}/d \log L dz$ and its one-dimensional projections (obtained by integrating over z or $\log L$) as predicted by a model with a lifetime distribution $f(\tau) \propto 1/\tau$ and an SFH of the form given by eq. (7). The luminosity function is a broken power law with $\alpha_1 = 1.5$ and $\alpha_2 = 2.5$ and $L_* = 2 \times 10^{51} \text{ erg s}^{-1}$, chosen to fit the BATSE $\log N - \log S$ distribution. The threshold of *Swift* is taken as a step function at 1 photon $\text{cm}^{-2} \text{ s}^{-1}$. The three *Swift* SHBs are marked with dots (on the two-dimensional plot) and bars (in the two projections). This model is rejected at 99.9% confidence level. [See the electronic edition of the *Journal* for a color version of this figure.]

of the two-dimensional distribution, which contains more information than the redshift distribution alone. This sample is, however, much more vulnerable to unaccounted errors.⁹

Figures 4 and 5 depict the predicted two-dimensional distributions of a power-law lifetime distribution with $\eta = -1$ and a narrow lognormal lifetime distribution with $\tau_* = 3 \text{ Gyr}$, respectively. These figures include also the observed distribution and the two one-dimensional projections of the models and the observations. The figures show clearly that even though there are only three observed SHBs in this sample, the two models do not describe the data well. Indeed both models are rejected at a confidence level that is larger than 99%.

This result can be understood. Given the intrinsic rate evolution $R_{\text{SHB}}(z)$ predicted by lifetime distributions with short delay ($< 3 \text{ Gyr}$) or small power-law index ($\eta < -0.5$), the luminosity function (eq. [9]) implies that the typical observed burst luminosity is L_* , and the typical observed redshift is the redshift at which L_* is detected at the threshold level.¹⁰ Regardless of the exact value of α_1 and α_2 , we find a typical luminosity $L_* \gtrsim 10^{51}$. Similar values of L_* were obtained by Ando (2004) for various luminosity functions. The typical redshift is $z \approx 0.7$, and together with L_* these two values are too high for the *Swift* sample. Longer lifetimes result in $R_{\text{SHB}}(z)$ that increases at low redshifts, leading to a lower value of L_* and to lower typical redshifts. For example, a delay of 6 Gyr results in $L_* = 4 \times 10^{50} \text{ erg s}^{-1}$ and predicts a distribution that is fully consistent with the observations (see Fig. 6).

Finally, we discuss the robustness of our limit on the progenitor lifetime in the case of a luminosity function of an arbitrary form. The reason that short lifetime models fail is the deficit of low-luminosity SHBs at low redshifts. In order to increase this fraction, the luminosity function must increase more steeply than L^{-2}

⁹ Repeating the analysis when the redshift of SHB 0508013 is taken as a lower limit > 0.72 (instead of equal to 0.72) does not alter the main results, i.e., that a long lifetime is required. The most likely values of τ_* and η are similar while $\tau_* < 1 \text{ Gyr}$ is rejected at 99.7% and $\eta < -1$ is rejected at 99.4%.

¹⁰ This statement is correct as long as L_* is detected up to a redshift $\lesssim 1$, which is the case for the values of L_* that we find and the *Swift* threshold.

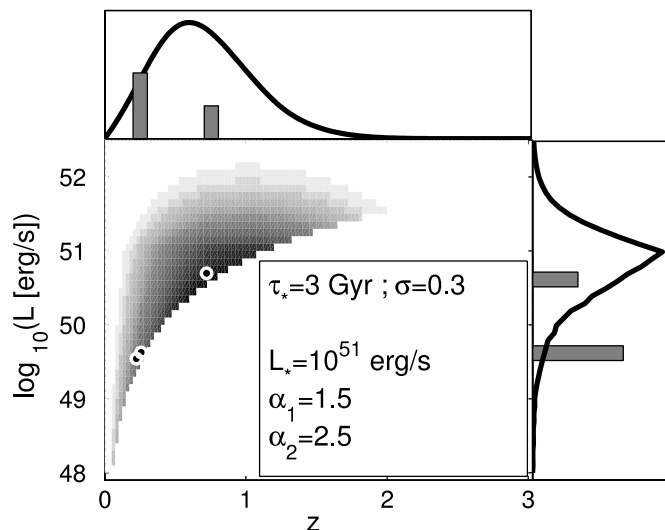


FIG. 5.—Same as Fig. 4, but for a model with a lognormal lifetime distribution ($\tau_* = 3 \text{ Gyr}$ and $\sigma = 0.3$) and $L_* = 10^{51} \text{ erg s}^{-1}$ (the rest of the parameters are the same as in Fig. 4). This model is rejected at 99% confidence level. [See the electronic edition of the *Journal* for a color version of this figure.]

at low luminosities ($\lesssim 10^{50} \text{ erg s}^{-1}$). In this case, however, the luminosity function must become flatter than L^{-2} at higher luminosities in order to fit the BATSE $\log N - \log S$ (i.e., the luminosity function must have an “ankle”). Although we cannot exclude a luminosity function with an ankle, and thus the possibility of a shorter typical lifetime, such a luminosity function is not expected unless SHBs are composed of two separate populations.

An alternative method to estimate the progenitor lifetime is based on the spectral types of the host galaxies (Gal-Yam et al. 2005). In the extended sample four out of the six putative host galaxies are of early type.¹¹ If only *Swift* and *HETE-2* bursts are considered, then three out of four are of early type. The two late-type galaxies are moderately star forming.¹² In one a significant fraction of the stars is $\sim 1 \text{ Gyr}$ old (SHB 050709; Covino et al. 2006). In the other most of the stars are much older than 1 Gyr (SHB 000607; Gal-Yam et al. 2005). Using these results, Gal-Yam et al. (2005) find that SHBs are more likely to reside in early-type galaxies than Type Ia SNe (at 2σ c.l.), implying that the typical lifetime of SHB progenitors is most likely longer than the one of Type Ia SNe ($> 1 \text{ Gyr}$). This method does not depend on the luminosity function or the instrumental thresholds and thus constitutes an independent corroboration of our results.

3.2. The Local Rate of SHBs

The most robust lower limit on the local SHB rate is obtained directly from the BATSE observed rate (a full sky rate of $\approx 170 \text{ yr}^{-1}$). Considering a single power-law luminosity function, the observed redshift distribution of the extended sample (eight bursts) should be similar to the BATSE redshift distribution of BATSE bursts.

¹¹ Note that the host of SHB 050813 is of early type regardless of whether it is associated with the cluster at $z = 0.72$ (Gladders et al. 2005; Berger 2005; Prochaska et al. 2005) or with a cluster at $z \approx 1.8$ (Berger 2006). Moreover, if the burst is truly associated with a cluster at $z \approx 1.8$, then the lifetime of its progenitor is $\approx 3 \text{ Gyr}$. It cannot be older since this is the age of the universe at this redshift, and it is not much younger since it is associated with one of the most developed, and therefore one of the oldest, structures at this redshift.

¹² Note that as we discuss in § 3, the host of SHB 051221 cannot be included in this sample without accounting for selection effects that prevent the detection of the hosts of other SHBs that were localized after we defined our sample. This is especially important when the host type is considered since we expect afterglows to be bright in gas-rich environments, making the identification of a late-type host more probable.

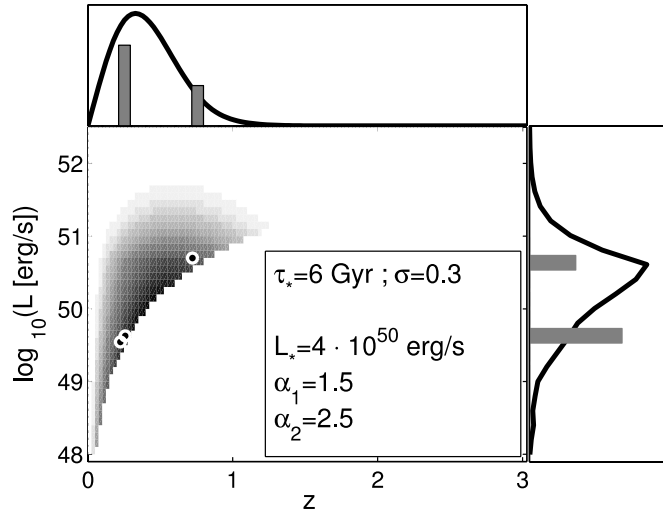


FIG. 6.— Same as Fig. 4, but for a model with a lognormal lifetime distribution ($\tau_* = 6$ Gyr and $\sigma = 0.3$) and $L_* = 4 \times 10^{50}$ ergs s^{-1} (the rest of the parameters are the same as in Fig. 4). This model provides a good description of the data. [See the electronic edition of the *Journal* for a color version of this figure.]

Therefore, the fact that five out of the eight bursts are within a distance of 1 Gpc suggests that the rate of SHBs observed by BATSE is ≈ 25 Gpc $^{-3}$ yr $^{-1}$ and puts a lower limit of ≈ 12 (6) Gpc $^{-3}$ yr $^{-1}$ at 2σ (3σ) confidence level. Even with no assumptions about the luminosity function, the sample of SHBs detected by *Swift* (three bursts), which has a comparable threshold to that of BATSE, gives a similar result. Two of these bursts are within 1 Gpc, suggesting the same rate of ≈ 25 Gpc $^{-3}$ yr $^{-1}$ and setting a lower limit of ≈ 6 (1) Gpc $^{-3}$ yr $^{-1}$ at 2σ (3σ) confidence level. The rate of SHBs observed by BATSE is a strict lower limit since it does not include undetected SHBs. Bursts can avoid detection either by pointing away from us, if the prompt gamma-ray emission is beamed, or by being too dim. This robust lower limit is higher than previous estimates (Schmidt 2001; Ando 2004; Guetta & Piran 2005) by a factor of 10–100. This observed local rate is also higher by the same factor than the observed local rate of long-soft GRBs (Schmidt 1999; Guetta et al. 2005).

The progenitors of SHBs are almost certainly a product of at least one core-collapse SN (e.g., a neutron star), and the SHB itself is most likely a catastrophic event; therefore, the rate of SHBs is limited by the rate of core-collapse SNe. Since we find that the typical lifetime of SHB progenitors is several billion years, the local rate of SHBs is limited by the rate of core-collapse SNe at a redshift ≈ 0.7 (Dahlen et al. 2004). Together with the observed lower limit, we find that the local rate of SHBs, $\mathcal{R}_{\text{SHB}} \equiv \mathcal{R}_{\text{SHB}}(z = 0)$, is in the range

$$10 \text{ Gpc}^{-3} \text{ yr}^{-1} \lesssim \mathcal{R}_{\text{SHB}} \lesssim 5 \times 10^5 \text{ Gpc}^{-3} \text{ yr}^{-1}. \quad (10)$$

Constraining the local rate within this range requires an estimate of the beaming factor (i.e., the fraction of the 4π solid angle into which the prompt gamma rays are emitted), f_b^{-1} , and of the luminosity function. The value of the beaming factor is currently unknown; however, the afterglows of two SHBs (050709 and 050724) have shown a steepening that can be interpreted as a hint of a jet (Fox et al. 2005). This interpretation, although somewhat speculative at this point, indicates a beaming factor of ~ 50 . The correction for undetected dim bursts depends on the luminosity function and most strongly on its lower cutoff, L_{\min} . Taking the power-law luminosity function that we have found above

$[\phi(L) \propto L^{-2}]$, the local rate is weakly sensitive to the exact evolution of \mathcal{R}_{SHB} with redshift (as long as the fraction of nearby bursts is compatible with the current sample¹³):

$$\mathcal{R}_{\text{SHB}} \approx 40 f_b^{-1} \left(\frac{L_{\min}}{10^{49} \text{ ergs s}^{-1}} \right)^{-1} \text{ Gpc}^{-3} \text{ yr}^{-1}. \quad (11)$$

Taking the beaming factor suggested by Fox et al. (2005; 30–50) and the value of L_{\min} suggested by our results in conjunction with the results of Tanvir et al. (2005; 10^{47} ergs s^{-1}), we obtain a rate of 10^5 Gpc $^{-3}$ yr $^{-1}$. This high rate is highly uncertain at this point, but we consider it to be the most favored by the synthesis of current observations. This rate is only slightly smaller than the upper limit we obtained (eq. [10]), implying that if this estimate is correct, a significant fraction of all of the end products of core-collapse SNe are producing SHBs. Alternatively, perhaps a source can produce more than a single SHB (i.e., SHBs are not catastrophic events). The upper limit that we find does not pose at the moment a stringent limit on the beaming or on L_{\min} . However, if in the future bursts with a luminosity of 10^{47} ergs s^{-1} will be observed, it will constrain the beaming to be smaller than ~ 100 .

4. SHBs AND COMPACT BINARY MERGERS

4.1. The Predicted Lifetime and Merger Rate of DNS and BH-NS Binaries

The merger rates of DNS and BH-NS systems are currently estimated in two ways, based on observed systems in our Galaxy and using theoretical population synthesis. Estimates based on observed DNS binaries (e.g., Phinney 1991; Narayan et al. 1991; Curran & Lorimer 1995; van den Heuvel & Lorimer 1996; Arzoumanian et al. 1999; Kalogera et al. 2001, 2004; de Freitas Pacheco et al. 2006) provide a lower limit on the local rate of DNS merger events because of possible unaccounted for selection effects (e.g., binary formation that does not recycle either of the neutron stars). The absence of observed BH-NS systems, together with poor understanding of selection effects involved in their discovery, renders this method inapplicable in this case. Population syntheses (e.g., Lipunov et al. 1995; Portegies Zwart & Yungelson 1998; Bethe & Brown 1998; Bloom et al. 1999a; Fryer et al. 1999; Belczynski & Kalogera 2001; Belczynski et al. 2002a, 2002b; Perna & Belczynski 2002) do not suffer from observational selection effects and can address both DNS and BH-NS binaries. However, the uncertainties involved are substantial, with rate estimates spanning over 3 orders of magnitude.

The estimates based on observed DNS systems were drastically revised with the discovery of the relativistic binary pulsar PSR J0737–3039 (Burgay et al. 2003). Based on three observed DNS binaries,¹⁴ Kalogera et al. (2004) find a range of Galactic merger rates from 1.7×10^{-5} to 2.9×10^{-4} yr $^{-1}$ at 95% confidence. This estimate is larger by a factor of 6–7 than the estimates that they obtained excluding PSR J0737–3039. Extrapolation of this rate to the cosmological neighborhood (Kalogera et al. 2004) yields LIGO-I and LIGO-II detection rates of 7×10^{-3} – 0.1 yr $^{-1}$ and 40–650 yr $^{-1}$, respectively. This rate corresponds to a local rate density of 200–3000 Gpc $^{-3}$ yr $^{-1}$.

Regardless of the exact values of the above-estimated rate, the merger rate for observed DNS binaries is dominated by systems

¹³ The rate varies by $\approx 30\%$ when calculated using the most likely values of the three models that we consider. Adopting values of the models that are rejected at 2σ (3σ) can reduce the rate by a factor of 3 (6).

¹⁴ Kalogera et al. (2004) consider only the observed DNS systems that will merge within a Hubble time. They further exclude PSR B2127+11C because of its association with a globular cluster.

with short lifetimes. This is demonstrated, for example, by the fact that the detection of PSR J0737–3039 (with a merger timescale of ≈ 100 Myr) significantly increased the estimated merger rate (Kalogera et al. 2004). Note that this drastic revision in the rate is partially due to the short lifetime of this double pulsar. Numerous new binaries with long lifetimes need to be discovered if old binaries are to dominate the merger rate in our Galaxy.

The rates found by population syntheses for DNS systems are in general consistent with the rate deduced from the observations. Analysis of BH-NS binaries shows that their merger rate may be comparable to, or even larger by an order of magnitude than (Bethe & Brown 1998), the rate of DNS mergers. Population synthesis provides a rather robust upper limit on the rate of DNS and BH-NS mergers by considering the fraction of binaries that survive two core-collapse SNe. Several theoretical works (e.g., Pfahl et al. 2002; Lipunov et al. 1997) show that this fraction is likely to be ~ 0.001 and can be as high as 0.02. Taking this fraction from the local rate of core-collapse SNe (Cappellaro et al. 1999) implies an upper limit of $1000 \text{ Gpc}^{-3} \text{ yr}^{-1}$ on the merger rate of short-lived binaries ($\tau \lesssim 1$ Gyr). An upper limit of $10^4 \text{ Gpc}^{-3} \text{ yr}^{-1}$ on the merger rate of long-lived binaries ($\tau \gtrsim 4$ Gyr) is obtained by considering the rate of core-collapse SNe at redshift 0.7 (Dahlen et al. 2004).

4.2. Comparison with SHBs

DNS or BH-NS mergers are currently the most popular models for SHBs (e.g., Eichler et al. 1989; Narayan et al. 1992). The proposed association is based on the tight limits that are imposed on the progenitor by the large energy release ($\sim 10^{50}$ ergs) and the short timescales (~ 1 ms) observed in these bursts. Not many sources can produce such an electromagnetic display, while an extensive numerical effort (e.g., Ruffert & Janka 1999; Janka et al. 1999; Rosswog et al. 2003; Lee et al. 2005; Oechslin & Janka 2006) has shown that the mergers of DNS and BH-NS systems can.

The range of SHB rates that we find (eq. [11]) overlaps the predicted rate of DNS mergers based on observations ($\sim 200\text{--}3000 \text{ Gpc}^{-3} \text{ yr}^{-1}$). However, the range of progenitor lifetimes we find for SHBs is inconsistent with that of the observed DNS binaries. The reason is that the merger rate of the latter is dominated by short-lived binaries ($\tau \sim 100$ Myr) while SHB progenitors are much older ($\tau \gtrsim 4$ Gyr). We do not see any obvious selection effect that may operate and can be applied to the current DNS models and explain this discrepancy. On the contrary, while very tight DNS binaries (with very short lifetimes) can avoid detection in pulsar surveys because of their large orbital accelerations, long-lived systems are detected with relative ease as long as one of the neutron stars is an active pulsar.

Admittedly, the probability that both members of a DNS binary are dead pulsars (i.e., undetectable) increases with its age. However, our limits on the lifetime distribution of SHBs constrain it to be shallower than $\tau^{-0.5}$ (at 95% c.l.). In other words, the number of newly born SHB progenitors with a lifetime between 1 and 10 Gyr is larger by a factor $\gtrsim 10$ than those with lifetime 10–100 Myr. Therefore, if DNS binaries are the progenitors of SHBs, for every recently born DNS with a lifetime 10–100 Myr we expect to observe at least several recently born systems with a lifetime of 1–10 Gyr. All of these coeval systems are presumably equally detectable via pulsar surveys. In reality there is one observed DNS with a lifetime of 10–100 Myr and only one with a lifetime of 1–10 Gyr (B1534+12, which is most likely older than 100 Myr). We therefore conclude that with the caveat of small number statistics, the observed population of DNS systems is unlikely to be the dominant component among SHB progenitors.

It is possible that known DNS pulsars are not representative of the larger population of relativistic DNS systems. This might be the case if large numbers of relativistic DNS systems are formed without recycled pulsars, or alternatively if the Milky Way DNS population does not represent the cosmic one. We thus conclude that SHB observations disfavor a DNS merger origin to the extent that they indicate that an unexpected hidden population of old long-lived systems should be invoked. While we cannot exclude the existence of such a population at the moment, it remains to be seen whether it can be reproduced by population synthesis models. Turning the argument around, if DNS binaries are the progenitors of SHBs, then there exists a large population of hitherto undetected old DNS systems. Moreover, this scenario suggests that the rate of SHBs is $\mathcal{R} \sim 10^3\text{--}10^4 \text{ Gpc}^{-3} \text{ yr}^{-1}$ in order to dominate over the merger rate of young DNS systems found by Kalogera et al. (2004), while conforming with the upper limit imposed by the rate of core-collapse SNe at $z \approx 0.7$ and the binary survival probability. It also excludes the existence of the recently hypothesized dominant population of DNS binaries with very short lifetimes (Belczyński & Kalogera 2001; Perna & Belczynski 2002).

The possibility that BH-NS systems are the dominant source of SHBs cannot be constrained at this time. There are no observational data on the properties of this population while the theoretical models are highly uncertain and their predictions vary significantly from one model to the next. If a link between SHBs and BH-NS mergers will be established in the future, the observed SHB properties can be used to constrain models of NS-BH binaries.

5. PROSPECTS FOR GRAVITATIONAL WAVE DETECTION

Progenitors of SHBs may also be strong sources of GWs. Therefore, the local SHB rate might have direct implications for the detection rate of GW telescopes in general and for the upcoming S5 run of initial LIGO (LIGO-I) in particular. The most promising progenitors for GW detection are NS-BH or DNS mergers. As we discuss above, our results disfavor, but cannot exclude, DNS binaries as the source of SHBs, while the possibility that NS-BH binaries are the progenitors on SHBs cannot be constrained by the data. Moreover, energy and timescale considerations favor compact binary mergers as the progenitors of SHBs. Therefore, it is worthwhile to discuss the predictions for the LIGO and VIRGO GW observatories if SHBs originate during such compact mergers.

These sources are expected to be detected by LIGO-I up to a distance of ~ 43 (20) Mpc (Cutler & Thorne 2002; hereafter the numbers without parentheses are for NS-BH mergers assuming a BH mass of $10 M_{\odot}$, while the numbers within the parentheses are for DNS mergers¹⁵). VIRGO design sensitivity¹⁶ is similar to that of LIGO-I; therefore, the VIRGO detection rate is expected to be similar once its design sensitivity is achieved. If SHBs are triggered by compact mergers, the prospects for GW detection from SHBs are quite promising. A reasonable, but speculative, SHB rate of $\sim 10^4 \text{ Gpc}^{-3} \text{ yr}^{-1}$ (see § 3.2) predicts a detection rate of ~ 3 (0.3) mergers yr^{-1} . This speculative rate is higher by a factor of ~ 10 than previous upper limits on merger rates derived from the local rate of core-collapse SNe. The reason is that the long lifetime of SHB progenitors relates them to SNe at redshift ~ 1 , which was higher by a factor of ~ 10 than it is today.

¹⁵ Recently Miller (2005) and Rosswog (2005) argued that BH-NS mergers with a mass ratio $\gtrsim 10$ cannot produce the accretion disk that is believed to be necessary for the production of SHBs. This result suggests that SHBs can be produced only by mergers of BHs and NSs with similar masses. In this case the W-detectability of BH-NS mergers is similar to that of DNS mergers.

¹⁶ See <http://www.virgo.infn.it/senscurve/>.

Possible temporal coincidence between an SHB and a GW signal may make the difference between detection and nondetection in the coming S5 run of LIGO-I. A coincident detection increases the range of LIGO-I and VIRGO by a factor of ≈ 1.5 , while if SHBs are preferentially beamed perpendicular to the binary orbital plane, the range is increased by an additional factor of ≈ 1.5 to a distance of ≈ 100 (50) Mpc (Kochanek & Piran 1993). Hence, LIGO-I has a nonnegligible probability to detect GWs simultaneously with a *Swift* detection of an SHB. Our best-fit model to the current observations [$\phi(L) \propto L^{-2}$, $L_{\min} < 10^{47}$ ergs s^{-1} , and any lifetime distribution that provides a large fraction of SHBs at low redshift] predicts that about 3% of the SHBs observed by BATSE are within 100 Mpc while about 1% are within 50 Mpc. Given that *Swift* detects ~ 10 SHBs yr^{-1} and that its threshold is comparable to that of BATSE, the expected rate of simultaneous detections of an SHB and a GW signal is ~ 0.3 (0.1) yr^{-1} . This rate depends on the beaming only through the assumption that SHBs are beamed perpendicular to the binary orbital plane. It could be further increased by a search for simultaneous GW signals and SHBs that are detected by *Swift* or the IPN but are not localized (such bursts are currently not announced and are not included in the *Swift* detection rate that we quote above).

Simultaneous detection of the inspiral GW signal from a compact merger and an SHB will provide conclusive evidence that SHBs originate from compact mergers and would improve our understanding of both merger physics and SHBs significantly. GWs can provide a unique view of the formation, and possibly the operation, of the inner engine powering burst, difficult to observe via any other observational method. If GWs from a merger are detected without a detected SHB, an association may still be secured by the detection of an on-axis orphan afterglow (Nakar & Piran 2003). The probability to detect an off-axis radio orphan afterglow as suggested by Levinson et al. (2002) is low unless the beaming is not significant. The reason is that the isotropic energy of an SHB that would be detected by LIGO-I or VIRGO is expected to be $\leq 10^{47}$ ergs, and if the beaming is significant, its total energy would be much lower, and the afterglow is expected to be too dim for detection by the time that the jet decelerates and spherical emission dominates.

Advanced LIGO (LIGO-II) would be able to detect NS-BH (DNS) mergers up to a distance of 650 (300) Mpc (Cutler & Thorne 2002). Thus, if SHBs originate in such mergers, then a robust lower limit for the detection of GWs by LIGO-II is 20 (2) yr^{-1} and the probable rate is larger by orders of magnitude. This rate is for detections of GW signals that are not associated with the prompt gamma-ray emission from an SHB. As discussed above, simultaneous detections will increase the LIGO-II range by a factor of 1.5–2.5 to ≈ 1.3 (0.6) Gpc (Kochanek & Piran 1993). So far, *HETE-2* observed one burst at a distance < 700 Mpc while *Swift* detected at least an additional two SHBs at distance ≤ 1 Gpc. The GBM detector on *GLAST*¹⁷ is expected to have a threshold that is similar to BATSE and more than half the sky field of view; thus, it is expected to detect at least five SHBs within a distance of 500 Mpc every year. The benefit of the simultaneous operation of LIGO-II and an efficient GRB detector goes beyond the high likelihood to observe simultaneous SHBs and mergers if they are associated: it will also be able to disprove the association at high significance if no simultaneous detection is observed.

SHBs may emit GWs also if the progenitor is not a compact binary merger. Any progenitor that involves the collapse of a rotating compact object to a black hole (e.g., the collapse of a rotating neutron star triggered by accretion; MacFadyen et al. 2005) will

produce GWs (see, e.g., Stark & Piran 1985). The amplitude of these waves is highly uncertain. Moreover, the absence of an accurate signal template will reduce its detectability. Such GW signals would most likely not be detected even by LIGO-II at distances much greater than 10 Mpc (Kokkotas & Stergioulas 2005 and references therein). If SHBs result from the collapse of a compact object that is not triggered by a merger, LIGO-II might detect several SHBs if they are significantly beamed and/or $L_{\min} \ll 10^{49}$ ergs s^{-1} .

6. CONCLUSIONS

We have extended previous analysis schemes (Piran 1992; Ando 2004; Guetta & Piran 2005), combining the observed peak flux distribution and the two-dimensional observed redshift-luminosity distribution of SHBs, to constrain their progenitor lifetime and their local rate. We apply this method to the extended sample of SHBs with redshift constraints presented in Gal-Yam et al. (2005). Our conclusions are as follows:

1. The progenitors of SHBs are dominated by an old population. If there is a typical lifetime, then it is $\tau_* > 4$ (1) Gyr at 95% (99.9%) confidence level. If the lifetime distribution is a power law with index η , then the number of progenitors per logarithmic lifetime interval increases significantly with lifetime: $\eta > -0.5$ (-1) at 95% (99.5%) confidence level. Similar results are obtained when only the *Swift* SHB sample is considered. These results were obtained assuming that the luminosity function and the lifetime distribution are unimodal.
2. We derive a lower limit on the local rate of SHBs, $\mathcal{R}_{\text{SHB,obs}} \gtrsim 10 \text{ Gpc}^{-3} \text{ yr}^{-1}$. This rate is comparable to the BATSE observed (all sky) rate and is a robust lower limit. It is obtained when we use the simplest luminosity function that fits the data, $\phi_L \propto L^{-2}$, or independently, if we take the *Swift* threshold to be comparable to that of BATSE, as implied by the SHBs observed by *Swift* so far, and consider only the *Swift* sample.
3. Assuming that SHB progenitors are the end products of core-collapse SNe and that they are catastrophic, we derive also a rate upper limit, the rate of core-collapse SNe at $z \approx 0.7$: $10 \text{ Gpc}^{-3} \text{ yr}^{-1} < \mathcal{R}_{\text{SHB}} < 5 \times 10^5 \text{ Gpc}^{-3} \text{ yr}^{-1}$.
4. Indications that SHBs are beamed (Fox et al. 2005) and that the luminosity function lower cutoff is $L_{\min} \ll 10^{49}$ ergs s^{-1} (§ 3.2; Tanvir et al. 2005) suggest that the local rate is much higher than our lower limit. Considering the current best, but highly uncertain, estimates of the beaming and L_{\min} , we get a local rate of $\mathcal{R}_{\text{SHB}} \approx 10^5 \text{ Gpc}^{-3} \text{ yr}^{-1}$.

We compare our constraints on the progenitors of SHBs to observational constraints on DNS mergers. We find that observed DNS binaries in our Galaxy are unlikely to be a representative sample of SHB progenitors. The reason is that the merger rate of the observed DNS binaries is dominated by short-lived systems ($\tau \lesssim 100$ Myr) while SHB progenitors are much older ($\tau \gtrsim 4$ Gyr). We are not aware of any obvious selection effect that would prevent the detection of recently formed yet long-lived DNS binaries; therefore, we conclude that our results disfavor DNS systems as the progenitors of SHBs. However, given the limited understanding of the formation of DNS systems and the possibility that some of the formation channels result in binaries that cannot be detected, we cannot exclude the possibility that DNS systems end their life as SHBs. If they do, then we expect a large number of undetected old DNS systems in our Galaxy. We consider also the theoretical constraints on BH-NS mergers and find that there are no robust constraints that prevent these from being the progenitors of SHBs (based on the lifetime and the rate), due to the uncertain properties of the BH-NS population.

¹⁷ See <http://f64.nsstc.nasa.gov/gbm/>.

If SHBs originate from either BH-NS or DNS mergers, then the prospects for detecting GWs by first-generation detectors and in the future planned advance LIGO (LIGO-II) are promising:

1. Our robust lower limit on the local rate of SHBs implies that LIGO-II will detect at least 20 merging BH and NS pairs with a mass ratio of a few, per year, if they are the progenitors of SHBs. A minimal rate of two DNS (or BH-NS with similar masses) mergers per year is predicted if these are the sources of SHBs. If an efficient GRB detector (e.g., *GLAST*) will be operational contemporaneously with LIGO-II, numerous simultaneous detections are expected. The absence of such detections will imply that compact binary mergers are not the progenitors of SHBs.

2. The highest possible rate of SHBs that is consistent with the upper limit on the merger rate of compact binaries ($10^4 \text{ Gyr}^{-3} \text{ yr}^{-1}$) predicts a LIGO-I and VIRGO detection rate of $\sim 3 \text{ yr}^{-1}$ if SHBs are mergers of BH-NS with a mass ratio of a few and $\sim 0.3 \text{ yr}^{-1}$ if they are DNS mergers or mergers of BH-NS with similar masses. This is the rate for GW detection only, with no associated SHB detection by *Swift*.

3. The predicted probability for a simultaneous detection of GWs by LIGO-I or VIRGO and an SHB by *Swift* in 1 yr of contemporary operation might not be negligible: $\sim 30\%$ for a BH-NS merger and $\sim 10\%$ for a DNS merger. This probability is derived assuming $\phi_L \propto L^{-2}$ with a lower luminosity cutoff $L_{\min} = 10^{47} \text{ ergs s}^{-1}$.

4. The probability for a simultaneous detection can be increased if a search for GW signals will be carried out at times that SHBs are detected, but not localized, by *Swift* or by any of the IPN spacecraft. If SHBs are not strongly beamed, this may significantly increase the probability of LIGO-I to detect a single event.

We are grateful to E. S. Phinney and E. Ofek for illuminating discussions and advice. We thank D. Frail, S. Kulkarni, R. Sari, B. Cameron, M. Milosavljević, H. Pfeiffer, D. Palmer, T. Piran, S. Ando, and C. Miller for helpful discussions. E. N. was supported by a senior research fellowship from the Sherman Fairchild Foundation. A. G. acknowledges support by NASA through Hubble Fellowship grant HST-HF-01158.01-A awarded by STScI, which is operated by AURA, Inc., for NASA, under contract NAS 5-26555.

REFERENCES

- Ando, S. 2004, *J. Cosmol. Astropart. Phys.*, 06, 007
- Arzoumanian, Z., Cordes, J. M., & Wasserman, I. 1999, *ApJ*, 520, 696
- Belczynski, K., Bulik, T., & Kalogera, V. 2002a, *ApJ*, 571, L147
- Belczynski, K., & Kalogera, V. 2001, *ApJ*, 550, L183
- Belczynski, K., Kalogera, V., & Bulik, T. 2002b, *ApJ*, 572, 407
- Berger, E. 2005, *GCN Circ.*, 3801, 1
- . 2006, in *AIP Conf. Proc.* 838, *Gamma-Ray Bursts in the Swift Era*, ed. S. S. Holt, N. Gehrels, & J. A. Nousek (Melville: AIP), 33
- Berger, E., et al. 2005, *Nature*, 438, 988
- Bethe, H. A., & Brown, G. E. 1998, *ApJ*, 506, 780
- Bloom, J. S., Kulkarni, S. R., & Djorgovski, S. G. 2002, *AJ*, 123, 1111
- Bloom, J. S., Sigurdsson, S., & Pols, O. R. 1999a, *MNRAS*, 305, 763
- Bloom, J. S., et al. 1999b, *Nature*, 401, 453
- . 2006, *ApJ*, 638, 354
- Burgay, M., et al. 2003, *Nature*, 426, 531
- Cappellaro, E., Evans, R., & Turatto, M. 1999, *A&A*, 351, 459
- Castro-Tirado, A. J., et al. 2005a, *A&A*, 439, L15
- . 2005b, *GCN Circ.*, 3673, 1
- Cobb, B. E., Bailyn, C. D., van Dokkum, P. G., Buxton, M. M., & Bloom, J. S. 2004, *ApJ*, 608, L93
- Covino, S., et al. 2006, *A&A*, 447, L5
- Curran, S. J., & Lorimer, D. R. 1995, *MNRAS*, 276, 347
- Cutler, C., & Thorne, K. S. 2002, preprint (gr-qc/0204090)
- Dahlen, T., et al. 2004, *ApJ*, 613, 189
- Dar, A. 2005a, *GCN Circ.*, 2942, 1
- . 2005b, preprint (astro-ph/0509257)
- de Freitas Pacheco, J. A., Regimbau, T., Vincent, S., & Spallicci, A. 2006, *Int. J. Mod. Phys. D*, 15, 235
- Efron, B. 1982, *The Jackknife, the Bootstrap and Other Resampling Plans* (Philadelphia: SIAM)
- Eichler, D., Livio, M., Piran, T., & Schramm, D. N. 1989, *Nature*, 340, 126
- Fox, D. B., et al. 2005, *Nature*, 437, 845
- Fryer, C. L., Woosley, S. E., & Hartmann, D. H. 1999, *ApJ*, 526, 152
- Gaensler, B. M., Slane, P. O., Gotthelf, E. V., & Vasisht, G. 2001, *ApJ*, 559, 963
- Galama, T. J., et al. 1998, *Nature*, 395, 670
- Gal-Yam, A., et al. 2004, *ApJ*, 609, L59
- . 2005, preprint (astro-ph/0509891)
- Gehrels, N., et al. 2005, *Nature*, 437, 851
- Ghirlanda, G., Ghisellini, G., & Celotti, A. 2004, *A&A*, 422, L55
- Gladders, M., Berger, E., Morrell, N., & Roth, M. 2005, *GCN Circ.*, 3798, 1
- Guetta, D., & Piran, T. 2005, *A&A*, 435, 421
- Guetta, D., Piran, T., & Waxman, E. 2005, *ApJ*, 619, 412
- Hjorth, J., et al. 2003, *Nature*, 423, 847
- . 2005a, *ApJ*, 630, L117
- . 2005b, *Nature*, 437, 859
- Hurley, K., et al. 2005, *Nature*, 434, 1098
- Janka, H.-T., Eberl, T., Ruffert, M., & Fryer, C. L. 1999, *ApJ*, 527, L39
- Kalogera, V., Narayan, R., Spergel, D. N., & Taylor, J. H. 2001, *ApJ*, 556, 340
- Kalogera, V., et al. 2004, *ApJ*, 601, L179
- Kochanek, C. S., & Piran, T. 1993, *ApJ*, 417, L17
- Kokkotas, K. D., & Stergioulas, N. 2005, preprint (gr-qc/0506083)
- Kouveliotou, C., Meegan, C. A., Fishman, G. J., Bhat, N. P., Briggs, M. S., Koshut, T. M., Paciesas, W. S., & Pendleton, G. N. 1993, *ApJ*, 413, L101
- Kulkarni, S. R., et al. 1998, *Nature*, 395, 663
- Lee, W. H., Ramirez-Ruiz, E., & Granot, J. 2005, *ApJ*, 630, L165
- Levan, A., & Tanvir, N. 2005, *GCN Circ.*, 3927, 1
- Levinson, A., Ofek, E. O., Waxman, E., & Gal-Yam, A. 2002, *ApJ*, 576, 923
- Lipkin, Y. M., et al. 2004, *ApJ*, 606, 381
- Lipunov, V. M., Postnov, K. A., & Prokhorov, M. E. 1997, *MNRAS*, 288, 245
- Lipunov, V. M., Postnov, K. A., Prokhorov, M. E., Panchenko, I. E., & Jorgensen, H. E. 1995, *ApJ*, 454, 593
- MacFadyen, A. I., Ramirez-Ruiz, E., & Zhang, W. 2005, preprint (astro-ph/0510192)
- Malesani, D., et al. 2004, *ApJ*, 609, L5
- Matheson, T., et al. 2003, *ApJ*, 599, 394
- Miller, M. C. 2005, *ApJ*, 626, L41
- Nakar, E., Gal-Yam, A., Piran, T., & Fox, D. B. 2006, *ApJ*, 640, 849
- Nakar, E., & Piran, T. 2003, *NewA*, 8, 141
- Narayan, R., Paczynski, B., & Piran, T. 1992, *ApJ*, 395, L83
- Narayan, R., Piran, T., & Shemi, A. 1991, *ApJ*, 379, L17
- Nomoto, K., & Kondo, Y. 1991, *ApJ*, 367, L19
- Oechslin, R., & Janka, H. 2006, *MNRAS*, 368, 1489
- Palmer, D. M., et al. 2005, *Nature*, 434, 1107
- Perna, R., & Belczynski, K. 2002, *ApJ*, 570, 252
- Pfahl, E., Rappaport, S., Podsiadlowski, P., & Spruit, H. 2002, *ApJ*, 574, 364
- Phinney, E. S. 1991, *ApJ*, 380, L17
- Piran, T. 1992, *ApJ*, 389, L45
- Porciani, C., & Madau, P. 2001, *ApJ*, 548, 522
- Portegies Zwart, S. F., & Yungelson, L. R. 1998, *A&A*, 332, 173
- Press, W. H., Teukolsky, S. A., Vetterling, W. T., & Flannery, B. P. 1992, *Numerical Recipes in C: The Art of Scientific Computing* (2nd ed.; Cambridge: Cambridge Univ. Press)
- Prochaska, J. X., Bloom, J. S., Chen, H.-W., Hansen, B., Kalirai, J., Rich, M., & Richer, H. 2005, *GCN Circ.*, 3700, 1
- Rosswog, S. 2005, *ApJ*, 634, 1202
- Rosswog, S., Ramirez-Ruiz, E., & Davies, M. B. 2003, *MNRAS*, 345, 1077
- Ruffert, M., & Janka, H.-T. 1999, *A&A*, 344, 573
- Saio, H., & Nomoto, K. 1985, *A&A*, 150, L21
- Schmidt, M. 1999, *ApJ*, 523, L117
- . 2001, *ApJ*, 559, L79
- Soderberg, A. M., et al. 2005, *ApJ*, 627, 877
- . 2006, preprint (astro-ph/0601455)
- Stancik, K. Z., et al. 2003, *ApJ*, 591, L17
- Stark, R. F., & Piran, T. 1985, *Phys. Rev. Lett.*, 55, 891
- Tanvir, N., Chapman, R., Levan, A., & Priddey, R. 2005, *Nature*, 438, 991
- Thomsen, B., et al. 2004, *A&A*, 419, L21
- van den Heuvel, E. P. J., & Lorimer, D. R. 1996, *MNRAS*, 283, L37